


Article

# Synthesis and Structure Characterization of Three Pharmaceutical Compounds Based on Tinidazole

Na Li <sup>1</sup>, Yuting Chen <sup>1</sup>, Ruixin Chen <sup>2,\*</sup>, Mingjuan Zhang <sup>1</sup>, Tingting Wu <sup>3</sup> and Kang Liu <sup>1,\*</sup> 

<sup>1</sup> Key Laboratory of Eco-Chemical Engineering, Ministry of Education, International Science and Technology Cooperation Base of Eco-Chemical Engineering and Green Manufacturing, College of Chemistry and Molecular Engineering, Qingdao University of Science and Technology, Qingdao 266042, China; ln583143362@163.com (N.L.); 15610579592@163.com (Y.C.); qustzmj@163.com (M.Z.)

<sup>2</sup> Department of Mathematics, College of Mathematics and Physics, Qingdao University of Science and Technology, Qingdao 266061, China

<sup>3</sup> College of Chemical Engineering, Qingdao University of Science and Technology, Qingdao 266042, China; ttwu@qust.edu.cn

\* Correspondence: mathcrx@163.com (R.C.); liukang82@126.com (K.L.)

**Abstract:** Tinidazole (TNZ), a 5-nitroimidazole derivative, has received increasing attention due to its pharmacological activities in treatment for amebic and parasitic infections. In this paper, we synthesized three novel drug supramolecular compounds successfully based on TNZ. The three compounds discussed were formed by TNZ and 2,6-dihydroxybenzoic acid (2,6-DHBA), 4-methylsalicylic acid (4-MAC), and 5-chloro-2-hydroxybenzoic acid (5-C-2-HBA). The N-H...O and O-H...O hydrogen bonds and weak C-H...O hydrogen bonds are the primary intermolecular forces in the construction of the three compounds. Crystal structure analysis revealed that all the compounds exhibit three-dimensional frameworks consisting of non-covalent interactions. Furthermore, six primary synthons, I R<sup>2</sup><sub>2</sub> (8), II R<sup>2</sup><sub>1</sub>(6), III R<sup>2</sup><sub>2</sub>(12), IV R<sup>3</sup><sub>3</sub>(9), V R<sup>2</sup><sub>2</sub>(12), VI R<sup>3</sup><sub>3</sub>(9), formed through various hydrogen bonds are found in the three compounds. Moreover, the resulting pharmaceutical supramolecular compounds show improved stability. Single-crystal X-ray diffraction analysis, infrared spectroscopy (IR), element analysis, and thermogravimetric analysis (TGA) are reported.

**Keywords:** tinidazole; supramolecule; intermolecular; cocrystals; synthon



**Citation:** Li, N.; Chen, Y.; Chen, R.; Zhang, M.; Wu, T.; Liu, K. Synthesis and Structure Characterization of Three Pharmaceutical Compounds Based on Tinidazole. *Crystals* **2023**, *13*, 947. <https://doi.org/10.3390/cryst13060947>

Academic Editors: José Gavira, Fiora Artusio and Rafael Contreras-Montoya

Received: 22 May 2023  
Revised: 7 June 2023  
Accepted: 7 June 2023  
Published: 12 June 2023



**Copyright:** © 2023 by the authors. Licensee MDPI, Basel, Switzerland. This article is an open access article distributed under the terms and conditions of the Creative Commons Attribution (CC BY) license (<https://creativecommons.org/licenses/by/4.0/>).

## 1. Introduction

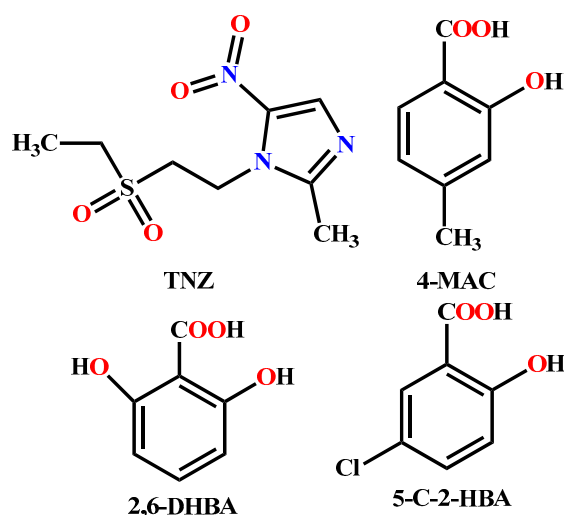
From extended research into molecular recognition and self-assembly, their chemistry has evolved from molecules to supramolecular chemistry that confers specific structure and function. Supramolecular chemistry is the science of studying the formation of functional systems formed by multiple molecules through non-covalent bonds [1–3]. In light of this, supramolecular chemistry is a widely accepted chemical discipline. Then, with the development of crystal engineering, solid cocrystals composed of two or more different molecules, generally in a stoichiometric ratio, have also been developed [4–6]. If at least one of the cocrystals is an active pharmaceutical ingredient (API) and the other is pharmaceutically acceptable in cocrystals, then it is recognized as a pharmaceutical cocrystal [7–9]. Pharmaceutical cocrystals have moved into the spotlight in research because they can improve the physicochemical properties of APIs, including as solubility, stability, and bioavailability, without changing the chemical integrity of the drugs [10,11]. Studies have reported improvements in dissolution rate by Rodríguez-Hornedo et al. [12], stability by Liu et al. [13], and bioavailability by Nangia et al. [14]. In the pharmaceutical field, cocrystals are composed of APIs and cocrystal formers (CCFs) via  $\pi$ - $\pi$  stacking interactions, intermolecular interactions, and hydrogen bonds [15–17]. Among these hydrogen bonds are the most significant forces in the formation of pharmaceutical supramolecules due to their stronger bond energies than other interactions [18–20]. Furthermore, APIs contain

inherent functional groups that can form supramolecular synthons through strong and weak hydrogen bonds, such as N-H...O, O-H...O, and C-H...O, which offer good support for the synthesis of pharmaceutical cocrystals [21–23].

Tinidazole (1-(2-(ethylsulfonyl)ethyl)-2-methyl-5-nitro-imidazol) is one of a group of nitromidazole derivative, which is an antiparasitic drug used as a treatment for a variety of amebic and parasitic infections and against most of the anaerobic periodontal pathogens, including five species of the genus *Prevotella*, *F. nucleatum*, and *Veillonella* spp [24–26]. Because of its important role in numerous pathological processes, TNZ has been widely studied in recent years. However, TNZ has low local bioactivity in the treatment of periodontal infections. Stability remains a key issue for a drug substance; therefore, improving the stability of drugs is also one of the main challenges for the pharmaceutical industry. In our work, we synthesized three pharmaceutical compounds and the stability was discussed.

From the perspective of crystal engineering, it is still a great challenge to prepare an ideal crystal material in accordance with the pre-designed connection mode and stoichiometric ratio due to the relatively weak and reversible properties of non-covalent intermolecular forces [27–31]. Therefore, methods to reasonably design cocrystals and salts with ideal structural characteristics and the selection of functional groups contained in the compound is essential. Aromatic carboxylic acids are a kind of organic supramolecular structural unit that can form stable skeleton structures through directed non-covalent forces (mainly hydrogen bonds); hence, it has attracted extensive attention of researchers [32,33]. In general, carboxylic acid ligands promote the self-association of supramolecular homosynthons (composed of the same complementary functional groups). In addition, aromatic carboxylic acids can also form stable supramolecular heterosynthons [composed of different but complementary functional groups (aromatic nitrogen, amide, etc.)]. In addition, the formation of cocrystals and salts is largely related to the solvent used. In this paper, we selected hydroxy-carboxylic acid as the main building unit to form supramolecular materials with TNZ. The main considerations are as follows: (i) this kind of carboxylic acid has two potential hydrogen bond donors: carboxyl—forming strong hydrogen bonds, and hydroxyl—forming weak hydrogen bonds. Therefore, it is expected that new supramolecular network structures may be formed with TNZ. (ii) TNZ has many C-H sites. Weak C-H...O bonds may be formed with carboxyl and hydroxyl groups. This weak C-H...O interaction plays a key role in enhancing the structural stability of supramolecules.

In this study, by using TNZ as the API, 2,6-DHBA, 4-MAC, and 5-C-2-HBA as CCFs, and acetone as the solvent, three novel TNZ-based pharmaceutical compounds connecting via various hydrogen bonds are prepared through the slow evaporation of solvents (Scheme 1). Moreover, their syntheses, structures, and thermal stabilities are reported.



Scheme 1. Molecular structures in this work.

## 2. Materials and Methods

### 2.1. General Materials and Methods

All the reagents and solvents utilized in our work were purchased commercially available and used as received without further purification. TNZ, 2,6-DHBA, 4-MAC, and 5-C-2HBA were obtained from Energy Chemical (Shanghai, China).

Melting point measurements were carried out using a WRS-1B digital thermal apparatus without correction and referred to the temperature at the start of the melt. The FT-IR absorption spectra were recorded on a Nicolet Impact 410 FTIR in the range of 4000–400  $\text{cm}^{-1}$  using the KBr pellets. TGA was performed from room temperature to 800 °C by using a Perkin-Elmer TGA-7 TG analyzer with a heating rate of 10 °C/min in a  $\text{N}_2$  atmosphere. The microanalyses of C, N, and H were performed on a Vario EL cube elemental analyzer.

### 2.2. Syntheses of the Compounds 1–3

In the process of solution crystallization, the solvent has an important effect on the crystal growth through the interaction with the crystal surface. Due to the solvo–surface interaction, the deposition of solute molecules on the crystal surface is hindered, that is, the relative growth rate of the corresponding surface is slowed down, which inhibits the growth of the crystal surface. Finally, the crystal morphology is affected by the relative growth rate of the crystal surface in different directions. The stronger the solvent–surface interaction, the slower the crystal surface grows, and the greater the influence of solvent on crystal growth. We used acetone as solvent to prepare high-quality crystals and the morphologies of all three compounds are rodlike crystals.

Synthesis of  $[(\text{C}_8\text{H}_{14}\text{N}_3\text{O}_4\text{S})\cdot(\text{C}_7\text{H}_5\text{O}_4)]$  (1) TNZ (0.0247 g, 0.10 mmol) and 2,6-DHBA (0.0154 g, 0.10 mmol) were taken into a mortar and mixed as much as possible. The mixture was ground together for 30 min in the mortar with a pestle. The resulting material was then dissolved in 5 mL acetone and the resulting solution was sealed in a 25 mL glass beaker with parafilm and kept at ambient temperature for crystallization through slow evaporation of the solvent. High-quality yellow rodlike crystals suitable for diffraction were obtained after two weeks as the solution slowly evaporated over at room temperature. The crystals were dried in vacuum to give the title compound. Crystals suited for single-crystal X-ray diffraction analysis were obtained by filtration. Yield: 70%. Anal. calcd for  $\text{C}_{15}\text{H}_{19}\text{N}_3\text{O}_8\text{S}$ : C, 44.88; H, 4.77; N, 10.47%. Found: C, 45.21; H, 4.97; N, 10.14%.

Synthesis of  $[(\text{C}_8\text{H}_{13}\text{N}_3\text{O}_4\text{S})\cdot(\text{C}_8\text{H}_8\text{O}_3)]$  (2) The preparation of compound 2 was similar to that of 1 except that 4-MAC (0.0152 g, 0.10 mmol) was used instead of 2,6-DHBA (0.0154 mg, 0.10 mmol). Yellow rodlike crystals in 1:1 stoichiometry ratio were obtained after 15 days when the solution was slowly evaporated at room temperature and dried under vacuum. Yield: 73%. Anal. calcd for  $\text{C}_{16}\text{H}_{21}\text{N}_3\text{O}_7\text{S}$ : C, 48.11; H, 5.30; N, 10.52%. Found: C, 48.60; H, 5.41; N, 10.21%.

Synthesis of  $[(\text{C}_8\text{H}_{13}\text{N}_3\text{O}_4\text{S})\cdot(\text{C}_7\text{H}_5\text{ClO}_3)]$  (3) A mixed solution of TNZ (0.0247 g, 0.10 mmol) and 5-C-2-HBA (0.0173 g, 0.10 mmol) was prepared with 5 mL acetone. Then the solution was placed in a magnetic stirrer and stirred for 30 min until a clear, homogeneous solution was obtained. Moreover, the resulting solution was left to slowly evaporate at ambient temperature. After 15 days, yellow rodlike crystals suitable for single crystal X-ray diffraction analysis were obtained. Then, the obtained crystals were dried under vacuum. Yield: 88%. Anal. calcd for  $\text{C}_{15}\text{H}_{18}\text{ClN}_3\text{O}_7\text{S}$ : C, 42.91; H, 4.32; N, 10.01%. Found: C, 43.14; H, 4.67; N, 9.86%.

We also used other carboxylic acids, such as 2-amino-6-hydroxybenzoic acid, 2-bromo-6-hydroxybenzoic acid, 3-chloro-2-hydroxybenzoic acid, and 2-hydroxyterephthalic acid in the synthesis process, but did not succeed in obtaining crystals. We proposed that this may be caused by the formation of unstable hydrogen bonds with TNZ.

### 2.3. X-ray Crystallography

The single crystal X-ray data for all crystals of suitable quality were collected on an Agilent Technologies (Santa Clara, CA, USA) Gemini A Ultra Atlas CCD with graphite monochromatic Mo-K $\alpha$  radiation ( $\lambda = 0.71073 \text{ \AA}$ ) at room temperature. Data collection and reduction were carried out through SMART and SAINT software [34]. All the structures were solved directly through SHELXS-97 software and refined by full-matrix least-squares techniques with anisotropic thermal parameters for all the non-hydrogen atoms on  $F^2$  with program SHELXL-97 [35] within Olex2 [36]. The structure diagrams were obtained by Diamond and Mercury software. Further details for crystallographic data and structural refinement parameters of the compounds are summarized in Table 1. The relevant hydrogen bond parameters are provided in Table 2.

**Table 1.** Crystal data and structure refinement summary for compounds 1–3.

Compound	1	2	3
Empirical formula	C <sub>15</sub> H <sub>19</sub> N <sub>3</sub> O <sub>8</sub> S	C <sub>16</sub> H <sub>21</sub> N <sub>3</sub> O <sub>7</sub> S	C <sub>15</sub> H <sub>18</sub> ClN <sub>3</sub> O <sub>7</sub> S
Formula weight	401.39	399.42	419.83
T/K	293(2)	293(2)	293(2)
Crystal system	monoclinic	triclinic	triclinic
Space group	Cc	$P_{-1}$	$P_{-1}$
a/Å	19.2461(9)	5.7197(3)	5.8506(4)
b/Å	11.1923(5)	11.0515(13)	11.0083(5)
c/Å	8.9518(4)	15.4804(12)	15.0294(9)
$\alpha/^\circ$	90	89.780(8)	92.248(4)
$\beta/^\circ$	115.967(4)	79.433(6)	101.203(5)
$\gamma/^\circ$	90	77.183(7)	103.511(5)
V/Å <sup>3</sup>	1733.62(15)	937.28(14)	919.61(10)
Z	4	2	2
$D_c/\text{g cm}^{-3}$	1.538	1.415	1.516
$\mu/\text{mm}^{-1}$	0.239	0.217	0.365
F(000)	840	420	436
Reflns collected	3679	6238	6058
Data/restraints/parameters	2090/2/248	3306/0/249	3229/0/248
S(GOF on $F^2$ )	1.059	1.095	1.069
h, k, lmax	18, 13, 10	6, 13, 13	5, 13, 17
R ( $I > 2\sigma(I)$ )	<sup>a</sup> $R_1 = 0.0285$ , <sup>b</sup> $wR_2 = 0.0617$	<sup>a</sup> $R_1 = 0.0511$ , <sup>b</sup> $wR_2 = 0.1127$	<sup>a</sup> $R_1 = 0.0366$ , <sup>b</sup> $wR_2 = 0.0922$
R (all data)	<sup>a</sup> $R_1 = 0.0310$ , <sup>b</sup> $wR_2 = 0.0634$	<sup>a</sup> $R_1 = 0.0859$ , <sup>b</sup> $wR_2 = 0.1375$	<sup>a</sup> $R_1 = 0.0474$ , <sup>b</sup> $wR_2 = 0.0998$

$$^a R_1 = \frac{\sum \Delta F_o \Delta - \Delta F_c \Delta}{\sum \Delta F_o \Delta}, \quad ^b wR_2 = \left[ \frac{\sum w(F_o^2 - F_c^2)^2}{\sum w(F_o^2)^2} \right]^{1/2}.$$

**Table 2.** Characteristics of hydrogen bond geometries observed in the crystal structures of 1–3.

	D–H...A (Å)	D–H(Å)	H...A(Å)	D...A(Å)	D–H...A (deg)
1	O1–H1...O2 (x, y, z)	0.820(1)	1.874(1)	2.598(1)	146.515(2)
	O4–H4...O3 (x, y, z)	0.820(1)	1.746(1)	2.480(1)	148.086(1)
	N2–H2...O2 (x, −1 − y, 0.5 + z)	0.860(1)	1.832(1)	2.681(1)	168.669(3)
	C11–H11B...O30 (x, −1 − y, 0.5 + z)	0.960(1)	2.146(1)	3.068(1)	160.688(2)
	C8–H8...O7 (x, −1 − y, 0.5 + z)	0.930(1)	2.396(1)	3.325(1)	176.673(2)
	C13–H13B...O4 (0.5 + x, −0.5 − y, 0.5 + z)	0.970(1)	2.417(1)	3.321(2)	154.897(4)
	O14A–H14A...O4 (0.5 + x, −0.5 − y, 0.5 + z)	0.970(1)	2.487(1)	3.384(1)	153.754(4)
2	O3–H3...O2 (x, y, z)	0.820(1)	1.914(2)	2.629(3)	145.206(9)
	O1–H1...N2 (−1 − x, 1 − y, 2 − z)	0.820(1)	1.886(2)	2.695(3)	168.959(1)
	C10–H10...O3 (1 + x, y, z)	0.930(1)	2.366(2)	3.260(2)	161.053(8)
	O3–H3...O2 (−x, 1 − y, 2 − z)	0.820(1)	2.441(3)	2.996(3)	125.84(12)
	C6–H6A...O3 (x, 1 + y, z)	0.975(0)	2.407(1)	3.286(2)	149.764(3)
	C14–H14B...O6 (1 + x, y, z)	0.970(1)	2.475(1)	3.403(2)	159.988(8)
	C14–H14A...O6 (x, y, z)	0.970(1)	2.578(3)	3.405(4)	143.210(1)
C16–H16C...O4 (2 + x, y, z)	0.960(1)	2.586(3)	3.469(4)	153.025(10)	

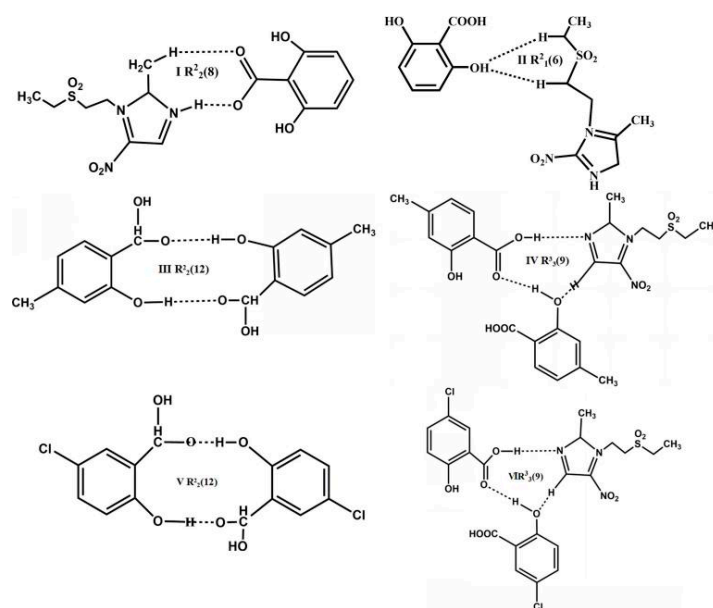
Table 2. Cont.

	D–H⋯A (Å)	D–H(Å)	H⋯A(Å)	D⋯A(Å)	D–H⋯A (deg)
3	O3–H3⋯O2 (x, y, z)	0.820(1)	1.897(1)	2.611(1)	145.061(7)
	O1–H1⋯N2 (1 – x, 1 – y, –z)	0.820(1)	1.866(1)	2.677(1)	169.912(7)
	C10–H10⋯O3 (–1 + x, y, z)	0.930(1)	2.371(1)	3.270(2)	162.369(6)
	O3–H1⋯O2 (–x, 1 – y, –z)	0.820(1)	2.491(2)	3.039(2)	125.248(7)
	C13–H13B⋯O6 (x, y, 1 + z)	0.970(1)	2.561(2)	3.385(2)	142.839(6)
	C13–H13A⋯O6 (x, y, z)	0.970(1)	2.539(2)	3.452(3)	156.959(5)
	C16–H16C⋯O4 (x, y, 1 + z)	0.960(1)	2.620(2)	3.424(2)	141.561(6)

Crystal data (excluding structure factors) for the structure in this paper have been deposited at the Cambridge Crystallographic Data Centre as supplementary publication no. CCDC 2256864–2256866. These data can be obtained free of charge via [www.ccdc.cam.ac.uk/conts/retrieving.html](http://www.ccdc.cam.ac.uk/conts/retrieving.html) (accessed on 6 June 2023). (or from the Cambridge Crystallographic Data Centre, 12 Union Road, Cambridge CB2 1EZ, UK; fax: (+44) 1223-336-033; or <https://deposit.ccdc.cam.ac.uk> (deposited on 17 April 2023)).

### 3. Results and Discussion

Three novel pharmaceutical compounds based on tinidazole and other common benzoic acids with different groups, including 2,6-dihydroxybenzoic acid (2,6-DHBA), 4-methylsalicylic acid (4-MAC), and 5-chloro-2-hydroxybenzoic acid (5-C-2-HBA), were prepared through a slow evaporation crystallization process (Table 1). These novel pharmaceutical compounds were analyzed by single-crystal X-ray diffraction, infrared spectroscopy, and thermogravimetric analysis. The results of single-crystal X-ray diffraction show the formation of three new compounds. The structural analysis of compounds 1–3 reveals multitudinous H-bond frameworks in which the tinidazole and carboxylic acids or carboxylic acid itself form numerous supramolecular synthons as shown in Scheme 2. Because of the large number of hydrogen bonds as weak forces, the structural rigidity and the thermal stability (original carboxylic acids vs. compounds) are significantly improved.



Scheme 2. The supramolecular synthons of 1–3.

#### 3.1. Molecular and Supramolecular Structural Descriptions of Compounds 1–3

Structural description of tinidazole: 2,6-dihydroxybenzoic acid 1:1 salt (1)

The single-crystal X-ray diffraction study reveals that compound **1** crystallizes in the *Cc* space group of the monoclinic system with  $Z = 4$ . As shown in Figure 1a, the asymmetric unit of compound **1** contains one deprotonated 2,6-DHBA with the H transferred to the N of the imidazole ring and one protonated TNZ. The exocyclic bond length C1–C2 is elongated to 1.478 Å, which is longer than the average cyclic C–C bond length of 1.382 Å. The deprotonated 2,6-DHBA anion and protonated TNZ cation form a dihedral angle of  $5.108^\circ$ .

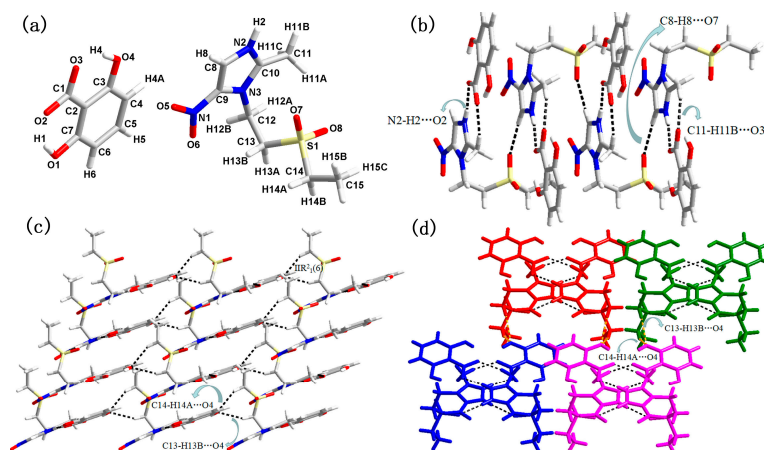


**Figure 1.** (a) Molecular structure of compound **1** with atom labels of the asymmetric unit. (b) The 1D supramolecular chain via hydrogen bonding interaction (the hydrogen bonds are indicated by broken lines in this and subsequent figures). (c) Perspective view of the 3D network along *ac* plane. (d) 3D network structure along *ab* plane.

As shown in Figure 1b, TNZ and 2,6-DHBA produced a heterodimer forming by the C11–H11...O3 (2.068 Å) and N2–H2...O2 (2.681 Å) hydrogen bonds. The dimer was extended further through the weak C8–H8...O7 (3.325 Å) non-classical interaction force established between SO<sub>2</sub> of TNZ and C–H donor of 2,6-DHBA with a C–O distance of 3.325(1) Å, forming a 1D chain structure. Within the 1D chain, the synthon I  $R^2_2(8)$  is discovered. Adjacent chains were linked through C13–H13B...O4 (3.321 Å) and C14–H14A...O4 (3.384 Å), forming a synthon II  $R^2_1(6)$  to construct a 3D net structure along the *ac* plane (Figure 1c). The 3D net structure along the *ab* plane is shown in Figure 1d.

Structural description of tinidazole: 4-methylsalicylic acid 1:1 cocrystal (**2**)

Compound **2** of TNZ-4-MAC crystallizes in the *P-1* space group of the triclinic system with  $Z = 2$ . The asymmetry unit of compound **2** (Figure 2a) contains one 4-MAC molecule and one TNZ molecule. The exocyclic bond length of C1–C2 and C5–C6 are elongated to 1.4616 Å and 1.5045 Å, which has an expanded C–C bond length compared with the cyclic C–C average bond length of 1.387 Å. The TNZ molecule and 4-MAC molecule are almost parallel due to their dihedral angle of  $1.6038^\circ$ .

Two 4-MAC were connected with two TNZ molecules through C10–H10...O3 (3.260 Å) between the C–H donor of TNZ and N of the imidazole ring, O1–H1...N2 (2.695 Å) between the carboxylic group and the N of imidazole ring, and O3–H3...O2 (2.996 Å) to construct a tetramer, which is centrosymmetric. Within the tetramer, III  $R^2_2(12)$ , IV  $R^3_3(9)$  were discovered. Two adjacent tetramers were connected together by the C14–H14B...O6 (3.403 Å) hydrogen bond to form a 2D single-layer structure (Figure 2c). Two adjacent 2D single-layer structures were further interlinked through the C14–H14A...O6 (3.405 Å) hydrogen bonding to form a 2D double-layer structure (Figure 2d). The space-filling model of the double-layer structure is shown in Figure 2e. The 2D double-layer structure is extended to form the 3D network structure through C16–H16C...O4 hydrogen bonds (Figure 2f).



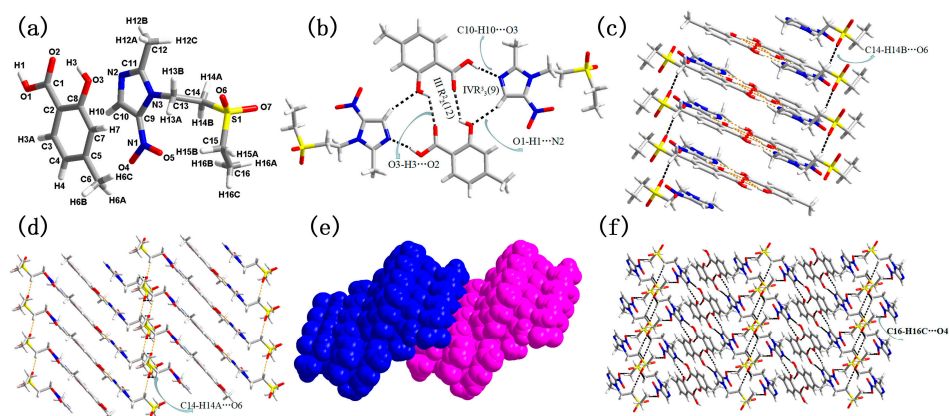


**Figure 2.** (a) Molecule structure of compound 2 with atom labels of the asymmetric unit. (b) The tetramer via hydrogen bonding interaction (the hydrogen bonds are indicated by broken lines in this and the subsequent figures). (c) Perspective view of the 2D single-layer; (d) 2D double-layer formed by adjacent single-layer. (e) The space-filling model of the double-layer structure. (f) The 3D network structure.

Structural description of tinidazole: 5-chloro-2-hydroxybenzoic acid 1:1 cocrystal (3)

The asymmetric unit of 3 (Figure 3a) contains a 5-C-2-HBA and a TNZ molecule. Single crystal X-ray diffraction revealed that compound 3 crystallizes in the *P*-1 space group of the triclinic system with *Z* = 2. The N3-C12-C13 angle of TNZ is 110.552°, the angle of C12-C12-S1 in TNZ is 113.067°, and the angles of C13-S1-C14 and S1-C14-C15 are 106.210° and 114.071°, respectively. The exocyclic bond length of C1-C2 is 1.471 Å, while the cyclic C-C average bond length is 1.384 Å in 5-C-2-HBA. The dihedral angle of 5-C-2-HBA and TNZ is 2.044°.

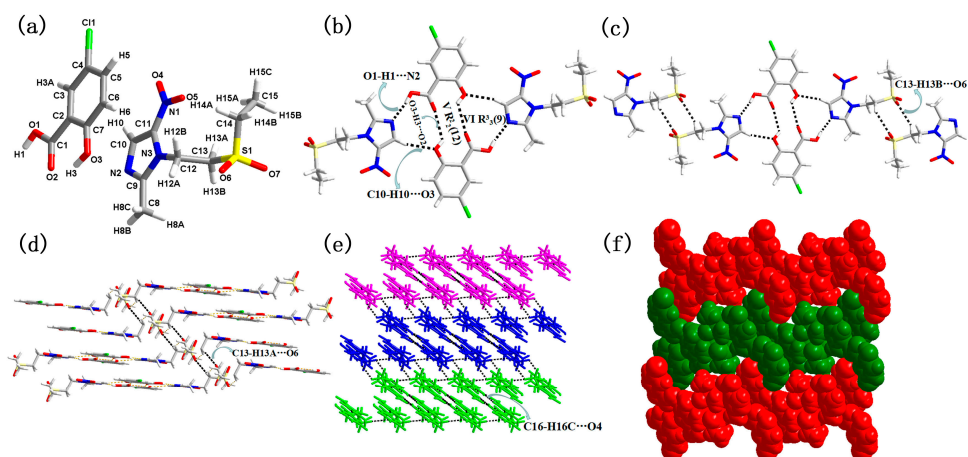


**Figure 3.** (a) Molecular structure of pharmaceutical supramolecular compound 3 with atom labels of the asymmetric unit. (b) The tetramer via hydrogen bonding interaction (the hydrogen bonds are indicated by broken lines in this and subsequent figures). (c) The 1D supramolecular chain via hydrogen bonding interaction. (d) Perspective view of the 2D hydrogen-bonded layer. (e) The 3D network structure. (f) The space-filling model of 3D structure.

Similar to compound 2, the 5-C-2-HBA homodimer and two TNZ molecular were connected to form a centrosymmetric tetramer (Figure 3a), which was joined together via O3-H3...O2 (2.611 Å) between the COO- and OH, O1-H1...N2 (2.677 Å) between the OH and the N of the imidazole ring, and the C10-H10...O10 (3.270 Å) hydrogen bonds. Within the tetramer, synthon  $V R^2_2$  (12) and  $VI R^3_3$  (9) appeared. The tetramer and TNZ molecule were connected via a C13-H13B...O6 (3.385 Å) non-covalent bond to generate an infinite 1D

chain structure (Figure 3c). In the 1D structure, the chain is propagated further through the C13-H13A...O6 (3.452 Å) non-classical interaction, forming a 2D layer structure (Figure 3d). In this case, the C13-H13A...O6 (3.452 Å) hydrogen bond is established between the CH<sub>2</sub> and the SO<sub>2</sub> with a C-O distance of 3.4523°. As shown in Figure 3e, the 2D layer structure is extended along the ab plane via C16-H16C...O4 hydrogen bond, forming the 3D structure, and the space-filling model clearly indicates the structure of the compound as displayed in Figure 3f.

### 3.2. Thermal Stability

All compounds 1–3 remain stable at normal temperature and pressure and can last for a long time. TGA was carried out to investigate the thermal properties of the three compounds between room temperature and 800 °C. The corresponding TGA curves are shown in Figure S2. For 2,6-DHBA, the TGA outcome shows that it remains stable until 182 °C with a slight weight loss between room temperature and 80 °C attributed to moisture absorption, and then a sharp weight loss ending at 204 °C; the total weight loss is 97.8%, corresponding to the decomposition of the carboxylic acid. For 4-MAC, the TGA result shows that it remains intact until 175 °C, and then there is a sharp weight loss ending at 200 °C and the total weight loss is 99.8%, corresponding to the decomposition of the carboxylic acid. For 5-C-2-HBA, the sample remains stable until 180 °C and then there is a sharp weight loss ending at 199 °C; the total weight loss is 99.7%, corresponding to the decomposition of the carboxylic acid. For TNZ, it can maintain stable until 225 °C and then structural collapse below 300 °C. As shown in Figure S2a, the temperature that weight loss occurs at in compound 1 is between pure 2,6-DHBA and TNZ, and the weight loss ratio is less than the pure TNZ and 2,6-DHBA, which indicates that the thermostability of compound 1 is improved compared with raw materials. Similarly, the stability of compounds 2 and 3 is also higher than that of the raw carboxylic acids shown in Figure S2b,c. Consequently, compounds 1–3 possess good stability compared with 2,6-DHBA, 4-MAC, and 5-C-2-HBA.

### 3.3. IR Analysis

Compared with the raw materials TNZ, 2,6-DHBA, 4-MAC, and 5-C-2-HBA, the characteristic peaks in compounds 1–3 are red-shifted or blue-shifted due to the formation of hydrogen bonds. For instance, the C = N [37] stretching band at 1642 cm<sup>-1</sup> and the characteristic peaks of the benzene ring [38] at 1585 cm<sup>-1</sup>, 1504 cm<sup>-1</sup>, and 1450 cm<sup>-1</sup> are respectively blue-shifted or red-shifted in compound 1 compared with the C = N stretching band of 1630 cm<sup>-1</sup> in pure TNZ or the characteristic framework vibrations peaks 1631 cm<sup>-1</sup>, 1579 cm<sup>-1</sup> and 1468 cm<sup>-1</sup> of the benzene ring in pure 2,6-DHBA. The IR analysis showed that compounds 1–3 are composed of TNZ and 2,6-DHBA, 4-MAC, and 5-C-2-HBA, respectively, and the interactions between them are hydrogen bonds, which was confirmed by the crystal structure analysis (Figure S1).

## 4. Conclusions

In this study, three compounds based on TNZ were obtained using 2,6-DHBA, 4-MAC, and 5-C-2-HBA via a simple solvent evaporation method and evaluated by single-crystal X-ray diffraction. The structure analysis indicates that hydrogen bonding plays a significant role in the supramolecular assemblies of tinidazole derivatives. It is clear from all the structures that this weak force plays a major role in stabilizing the structure once stronger hydrogen bonds are formed. The C-H...O interaction is present in all compounds, indicating that C-H is a ready hydrogen bond donor. Synthons (I R<sub>2</sub><sup>2</sup>(8), II R<sub>1</sub><sup>2</sup>(6) in 1, III R<sub>2</sub><sup>2</sup>(12), IV R<sub>3</sub><sup>3</sup>(9) in 2, V R<sub>2</sub><sup>2</sup>(12), VI R<sub>3</sub><sup>3</sup>(9) in 3) formed by various hydrogen bonds are the structural units that constitute the final 3D structures. Moreover, the stability of compounds 1–3 was significantly improved compared with aromatic carboxylic acids, which could be attributed to the existence of hydrogen bonding. TNZ was used to form cocrystals and salts



exhibiting improved apparent stability with CCFs via typical non-covalent bonds, which encourages further co-crystallization trials of TNZ with other CCFs.

**Supplementary Materials:** The following supporting information can be downloaded at: <https://www.mdpi.com/article/10.3390/cryst13060947/s1>, Figure S1: The IR spectras of 1–3; Figure S2: Thermogravimetric analysis (TGA) curves of compounds.

**Author Contributions:** Conceptualization, N.L. and K.L.; methodology, M.Z. and Y.C.; software, N.L. and Y.C.; validation, M.Z.; formal analysis, M.Z.; resources, T.W.; data curation, K.L.; writing—original draft preparation, N.L.; writing—review and editing, R.C.; visualization, T.W.; supervision, R.C.; project administration, T.W.; funding acquisition, K.L. All authors have read and agreed to the published version of the manuscript.

**Funding:** This work was supported by the National Natural Science Foundation of China (22002068; 52272222, and 52072197), Youth Innovation and Technology Foundation of Shandong Higher Education Institutions, China (2019KJC004), and the Natural Science Foundation of Shandong Province of China (ZR2022MB022).

**Data Availability Statement:** Data available on request from the authors.

**Conflicts of Interest:** The authors declare no conflict of interest.

## References

1. Bolla, G.; Sarma, B.; Nangia, A.K. Crystal Engineering of Pharmaceutical Cocrystals in the Discovery and Development of Improved Drugs. *Chem. Rev.* **2022**, *122*, 11514–11603. [[CrossRef](#)]
2. Surov, A.O.; Voronin, A.P.; Drozd, K.V.; Volkova, T.V.; Vasilev, N.; Batov, D.; Churakov, A.V.; Perlovich, G.L. Extending the Range of Nitrofurantoin Solid Forms: Effect of Molecular and Crystal Structure on Formation Thermodynamics and Physicochemical Properties. *Cryst. Growth Des.* **2022**, *22*, 2569–2586. [[CrossRef](#)]
3. Beletskaya, I.; Tyurin, V.S.; Tsvadze, A.Y.; Guillard, R.; Stern, C. Supramolecular Chemistry of Metalloporphyrins. *Chem. Rev.* **2009**, *109*, 1659–1713. [[CrossRef](#)]
4. Zhang, J.; Feng, Y.; Bo, Y.; Chinnam, A.K.; Singh, J.; Staples, R.J.; He, X.; Wang, K.; Zhang, J.; Shreeve, J.M. Synthesis of a high-energy-density material through rapid replacement of crystal water of hydrates. *Chem* **2022**, *8*, 2678–2687. [[CrossRef](#)]
5. Singh, M.; Liu, K.; Qu, S.; Ma, H.; Shi, H.; An, Z.; Huang, W. Recent Advances of Cocrystals with Room Temperature Phosphorescence. *Adv. Opt. Mater.* **2021**, *9*, 2002197. [[CrossRef](#)]
6. Bennion, J.C.; Matzger, A.J. Development and Evolution of Energetic Cocrystals. *Acc. Chem. Res.* **2021**, *54*, 1699–1710. [[CrossRef](#)] [[PubMed](#)]
7. Farooq, M.Q.; Abbasi, N.M.; Smith, E.A.; Petrich, J.W.; Anderson, J.L. Characterizing the Solvation Characteristics of Deep Eutectic Solvents Composed of Active Pharmaceutical Ingredients as a Hydrogen Bond Donor and/or Acceptor. *ACS Sustain. Chem. Eng.* **2022**, *10*, 3066–3078. [[CrossRef](#)]
8. Huang, Z.; Suzuki, H.; Ito, M.; Noguchi, S. Direct detection of the crystal form of an active pharmaceutical ingredient in tablets by X-ray absorption fine structure spectroscopy. *Int. J. Pharmaceut.* **2022**, *625*, 122057. [[CrossRef](#)] [[PubMed](#)]
9. Sugden, I.J.; Braun, D.E.; Bowskill, D.H.; Adjiman, C.S.; Pantelides, C.C. Efficient Screening of Coformers for Active Pharmaceutical Ingredient Cocrystallization. *Cryst. Growth Des.* **2022**, *22*, 4513–4527. [[CrossRef](#)] [[PubMed](#)]
10. Liu, L.; Yu, Y.; Bu, F.; Li, Y.; Yan, C.; Wu, Z. The First Cocrystallization of Milrinone with Nutraceuticals: The Adjusting Effects of Hydrophilicity/Hydrophobicity in Cavities on the In Vitro/In Vivo Properties of the Cocrystals. *Cryst. Growth Des.* **2022**, *22*, 1623–1637. [[CrossRef](#)]
11. Liu, Y.; Yang, F.; Zhao, X.; Wang, S.; Yang, Q.; Zhang, X. Crystal Structure, Solubility, and Pharmacokinetic Study on a Hesperetin Cocrystal with Piperine as Coformer. *Pharmaceutics* **2022**, *14*, 94. [[CrossRef](#)]
12. Good, D.J.; Rodriguez-Hornedo, N. Solubility Advantage of Pharmaceutical Cocrystals. *Cryst. Growth Des.* **2009**, *9*, 2252–2264. [[CrossRef](#)]
13. Liu, L.; Wang, J.; Mei, X. Enhancing the stability of active pharmaceutical ingredients by the cocrystal strategy. *Cryst. Eng. Comm.* **2022**, *24*, 2002–2022. [[CrossRef](#)]
14. Nangia, A.K.; Desiraju, G.R. Heterosynthons, Solid Form Design and Enhanced Drug Bioavailability. *Angew. Chem. Int. Ed.* **2022**, *61*, e202207484. [[CrossRef](#)] [[PubMed](#)]
15. Chen, X.; Ning, L. Pharmaceutical cocrystals of norgestrel acetate with superior dissolution. *CrystEngComm* **2022**, *24*, 6385–6391. [[CrossRef](#)]
16. Yang, Y.; Niu, H.; Xia, S.; Guo, Y.; Wu, X. Solubility and dissolution rate of progesterone cocrystals using 4-fluorobenzoic acid and 2-hydroxy-6-naphthoic acid as coformers. *J. Cryst. Growth* **2022**, *585*, 126601.
17. Riley, D.D.; Nicolas, J.V.; Aaron, D.F.; Venkata, S.M.; Manish, A.M. The Effects of Humidity on Spontaneous Cocrystallization: A Survey of Diacid Cocrystals with Caffeine, Theophylline, and Nicotinamide. *J. Chem. Crystallogr.* **2022**, *52*, 479–484.

18. Wang, L.; Luo, M.; Li, J.H.; Wang, J.M.; Zhang, H.L.; Deng, Z.W. Sweet Theophylline Cocrystal with Two Tautomers of Acesulfame. *Cryst. Growth Des.* **2015**, *15*, 2574–2578. [[CrossRef](#)]
19. Yao, J.; Chen, J.M.; Xu, Y.B.; Lu, T.B. Enhancing the Solubility of 6-Mercaptopurine by Formation of Ionic Cocrystal with Zinc Trifluoromethanesulfonate: Single-Crystal-to-Single-Crystal Transformation. *Cryst. Growth Des.* **2014**, *14*, 5019–5025. [[CrossRef](#)]
20. Nangia, A.; Rodriguez-Hornedo, N. Indo–U.S. Workshop on Pharmaceutical Cocrystals and Polymorphs. *Cryst. Growth Des.* **2009**, *9*, 3339–3341. [[CrossRef](#)]
21. Childs, S.L.; Zaworotko, M.J. The Reemergence of Cocrystals: The Crystal Clear Writing Is on the Wall Introduction to Virtual Special Issue on Pharmaceutical Cocrystals. *Cryst. Growth Des.* **2009**, *9*, 4208–4211. [[CrossRef](#)]
22. Zhang, X.M.; Tian, Y.Y.; Jia, J.T.; Zhang, T.T.; Zhu, G.S. Synthesis, characterization and dissolution of three pharmaceutical cocrystals based on deferiprone. *J. Mole Struct.* **2016**, *1108*, 560–566. [[CrossRef](#)]
23. Bathori, N.B.; Lemmerer, A.; Venter, G.A.; Bourne, S.A.; Caira, M.R. Pharmaceutical Co-crystals with Isonicotinamide-Vitamin B3, Clofibrac Acid, and Diclofenac—And Two Isonicotinamide Hydrates. *Cryst. Growth Des.* **2011**, *11*, 75–87. [[CrossRef](#)]
24. Wang, C.H.; Wang, F.; Li, C.Y.; Xu, X.L.; Li, T.; Wang, C.F. Voltammetric sensor for tinidazole based on poly(carmin) film modified electrode and its application. *Dyes Pigments* **2007**, *75*, 213–217. [[CrossRef](#)]
25. Rams, T.E.; Sautter, J.D.; van Winkelhoff, A.J. Comparative In Vitro Resistance of Human Periodontal Bacterial Pathogens to Tinidazole and Four Other Antibiotics. *Antibiotics* **2020**, *9*, 68. [[CrossRef](#)]
26. Pandiyan, R.; Vinothkumar, V.; Chen, T.; Chen, S.; Abinaya, M.; Rwei, S.; Hsu, H.; Huang, C.; Yu, M. Synthesis of Ag@ZrO<sub>2</sub> nanoparticles: A sensitive electrochemical sensor for determination of antibiotic drug tinidazole. *Int. J. Electrochem. Sci.* **2022**, *17*, 220414. [[CrossRef](#)]
27. Smirnov, A.S.; Mikherdov, A.S.; Rozhkov, A.V.; Gomila, R.M.; Frontera, A.; Kukushkin, V.Y.; Bokach, N.A. Halogen Bond-Involving Supramolecular Assembly Utilizing Carbon as a Nucleophilic Partner of I···C Non-covalent Interaction. *Chem.-Asian J.* **2023**, *18*, e202300037. [[CrossRef](#)] [[PubMed](#)]
28. Bosch, E.; Ferrence, G.M.; Powell, C.J.; Unruh, D.K.; Krueger, H.R., Jr.; Groeneman, R.H. Cooperative non-covalent interactions and synthetic feed as driving forces to structural diversity within organic co-crystals containing isosteric perhalobenzenes. *CrystEngComm* **2022**, *24*, 3841–3845. [[CrossRef](#)]
29. Singh, J.; Kim, H.; Chi, K. Non-Covalent Interaction-Directed Coordination-Driven Self-Assembly of Non-Trivial Supramolecular Topologies. *Chem. Rec.* **2021**, *21*, 574–593. [[CrossRef](#)]
30. Novikov, A.S. Non-Covalent Interactions in Organic, Organometallic, and Inorganic Supramolecular Systems Relevant for Medicine, Materials Science, and Catalysis. *Crystals* **2022**, *12*, 246. [[CrossRef](#)]
31. Mahmudov, K.T.; Kopylovich, M.N.; Guedes da Silva, M.F.C.; Pombeiro, A.J.L. Non-covalent interactions in the synthesis of coordination compounds: Recent advances. *Coordin. Chem. Rev.* **2017**, *345*, 54–72. [[CrossRef](#)]
32. Wu, Y.; Zhou, J.; Jin, S.; Liu, B.; Shi, C.; Wang, D. Preparation and structure analysis of non-covalent interactions mediated 2D-3D supramolecular adducts from 6-methylnicotinamide and carboxylic acids. *J. Mol. Struct.* **2022**, *1264*, 133135. [[CrossRef](#)]
33. Surov, A.O.; Voronin, A.P.; Vasilev, N.A.; Ilyukhin, A.B.; Perlovich, G.L. Novel cocrystals of the potent 1,2,4-thiadiazole-based neuroprotector with carboxylic acids: Virtual screening, crystal structures and solubility performance. *New J. Chem.* **2021**, *45*, 3034–3047. [[CrossRef](#)]
34. SMART and SAINT+ for Windows NT, Version 6.02a; Bruker Analytical X-ray Instruments Inc.: Madison, WI, USA, 1998.
35. Sheldrick, G.M. A short history of SHELX. *Acta Cryst. A* **2008**, *64*, 112–122. [[CrossRef](#)]
36. Dolomanov, O.V.; Bourhis, L.J.; Gildea, R.J.; Howard, J.A.K.; Puschmann, H.J. OLEX2: A complete structure solution, refinement and analysis program. *Appl. Cryst.* **2009**, *42*, 339–341. [[CrossRef](#)]
37. Tobón Zapata, G.E.; Martínez Carmona, D.M.; Echeverría, G.A.; Piro, O.E. Molecular structures of two copper complexes with the pharmaceuticals norfloxacin and tinidazole, when powder X-ray diffraction assists multi-domain single-crystal X-ray diffraction. *Acta Cryst. B* **2022**, *78*, 490–498. [[CrossRef](#)] [[PubMed](#)]
38. Fayaz, T.K.S.; Palanisamy, V.; Sanphui, P.; Chernyshev, V. Multicomponent solid forms of antibiotic cephalexin towards improved chemical stability. *CrystEngComm* **2023**, *25*, 1252–1262. [[CrossRef](#)]

**Disclaimer/Publisher's Note:** The statements, opinions and data contained in all publications are solely those of the individual author(s) and contributor(s) and not of MDPI and/or the editor(s). MDPI and/or the editor(s) disclaim responsibility for any injury to people or property resulting from any ideas, methods, instructions or products referred to in the content.